# Accepted Manuscript

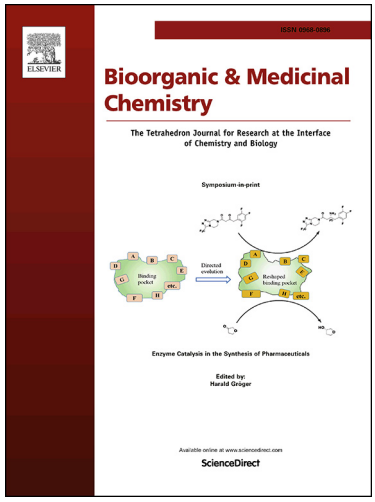


Synthesis and characterization of radioiodinated 3-phenethyl-2-indolinone derivatives for SPECT imaging of survivin in tumors

Natsumi Ishikawa, Takeshi Fuchigami, Tatsuya Mizoguchi, Sakura Yoshida, Mamoru Haratake, Morio Nakayama

PII: S0968-0896(18)30057-9
DOI: https://doi.org/10.1016/j.bmc.2018.04.034
Reference: BMC 14317

To appear in: *Bioorganic & Medicinal Chemistry*

Received Date: 12 January 2018
Revised Date: 11 April 2018
Accepted Date: 16 April 2018

Please cite this article as: Ishikawa, N., Fuchigami, T., Mizoguchi, T., Yoshida, S., Haratake, M., Nakayama, M., Synthesis and characterization of radioiodinated 3-phenethyl-2-indolinone derivatives for SPECT imaging of survivin in tumors, *Bioorganic & Medicinal Chemistry* (2018), doi: https://doi.org/10.1016/j.bmc.2018.04.034

# Synthesis and characterization of radioiodinated 3-phenethyl-2-indolinone derivatives for SPECT imaging of survivin in tumors

Natsumi Ishikawa[a], Takeshi Fuchigami[a]*, Tatsuya Mizoguchi[a], Sakura Yoshida[a], Mamoru Haratake[b], Morio Nakayama[a]*

[a] Department of Hygienic Chemistry, Graduate School of Biomedical Sciences, Nagasaki University, 1-14 Bunkyo-machi, Nagasaki 852-8521, Japan

[b]Faculty of Pharmaceutical Sciences, Sojo University, 4-22-1 Ikeda, Kumamoto 860-0082, Japan

*corresponding author:

Takeshi Fuchigami,

Graduate School of Biomedical Sciences, Nagasaki University, 1-14 Bunkyo-machi, Nagasaki 852-8521, Japan.

Tel.: +81-95-819-2443;

Fax: +81-95-819-2443;

E-mail: t-fuchi@nagasaki-u.ac.jp

Morio Nakayama,

Graduate School of Biomedical Sciences, Nagasaki University, 1-14 Bunkyo-machi, Nagasaki 852-8521, Japan.

Tel.: +81-95-819-2441;

Fax: +81-95-819-2441;

E-mail: morio@nagasaki-u.ac.jp

**Abstract**

Survivin, overexpressed in most cancers, is associated with poor prognosis and resistance to radiation therapy and chemotherapy. Herein, we report the synthesis of three 3-phenethyl-2-indolinone derivatives and their application as *in vivo* imaging agents for survivin. Of these, 3-(2-(benzo[d][1,3]dioxol-5-yl)-2-oxoethyl)-3-hydroxy-5-iodoindolin-2-one (IPI-1) showed the highest binding affinity ($K_d$ = 68.3 nM) to recombinant human survivin, as determined by quartz crystal microbalance (QCM). *In vitro* studies demonstrated that the [$^{125}$I]IPI-1 binding in survivin-positive MDA-MB-231 cells was significantly higher than that in survivin-negative MCF-10A

cells. In addition, uptake of [$^{125}$I]IPI-1 by MDA-MB-231 cells decreased in a dose-dependent manner in the presence of the high-affinity survivin ligand S12; this is indicative of specific binding of [$^{125}$I]IPI-1 to cellular survivin protein *in vitro*. Biodistribution studies in MDA-MB-231 tumor-bearing mice demonstrated the moderate uptake of[$^{125}$I]IPI-1 in the tumor tissue (1.37% ID/g) at 30 min that decreased to 0.32% ID/g at 180 min. Co-injection of S12 (2.5 mg/kg) slightly reduced tumor uptake and the tumor/muscle ratio of [$^{125}$I]IPI-1. Although further structural modifications are necessary to improve pharmacokinetic properties, our results indicate that PI derivatives may be useful as tumor-imaging probes targeting survivin.

**Key words**: survivin, cancer imaging, single photon emission computed tomography (SPECT).

## 1. Introduction

Survivin, the smallest protein (16.5 kDa) of the inhibitor of apoptosis protein (IAP) family, is highly expressed in several cancers but shows undetectable expression in non-dividing tissues.[1,2] The expression of survivin contributes to the resistance against chemotherapy and radiotherapy and is associated with the malignancy and prognosis in cancer patients.[3] This protein forms a homodimer or heterometric complexes with various proteins with multifunctional roles, including cancer survival, proliferation, progression, and angiogenesis.[4-6] As survivin has been proposed to be an ideal target for the specific diagnosis and treatment of most cancer types, various anticancer agents and intervention targeting survivin have been developed, including small-molecules, antisense oligonucleotides, and vaccines.[7-10] Radioligands such as $^{99m}$Tc-labeled antisense oligonucleotide targeting survivin mRNA have been developed for the diagnosis of cancer; however, these agents have limitations such as the lack of *in vivo* metabolic stability and specificity.[11] We recently reported a radioiodinated 4,6-diaryl-3-cyano-2-pyridinone derivative ([$^{125}$I]IDCP) that directly binds to survivin and demonstrated its application in single-photon emission computed tomography (SPECT) imaging of survivin (Fig. 1).[12] [$^{125}$I]IDCP exhibited significantly higher accumulation in MDA-MB-231 cells that display high expression of survivin as

compared with MCF-10A cells with low expression of survivin. However, the biodistribution study of [$^{125}$I]IDCP in tumor-bearing mice revealed its inadequate uptake by the cancer tissue.

In our continuing effort to explore more useful chemical backbones, we selected 3-phenethyl-2-indolinone (PI) as a new core structure for survivin imaging. PI derivative S12 (Fig. 1) has been reported to exhibit high binding affinity for survivin dimer interface ($K_a = 447 \times 10^6\ M^{-1}$) and inhibit tumor growth *in vitro* and *in vivo* based on survivin degradation.[13] Nuclear magnetic resonance (NMR) analysis of S12 and survivin-binding interaction showed that the bromine atom of S12 with other hydrophobic functional groups maintained its binding affinity for survivin. We designed an iodine analog of PI (IPI-1), wherein the bromine atom was replaced with an iodine atom at position 5 of S12 for its application as a SPECT imaging probe (Fig. 2). In addition, benzo[1,3]dioxolyl group at the 3-position of PI backbone was replaced with dimethoxyphenyl or benzoxazolyl group. Thus, we designed IPI-2 and IPI-3 as new candidate agents for survivin imaging (Fig. 2).

In this study, we performed the synthesis of IPI derivatives and radioiodination and evaluated their efficiencies as *in vivo* imaging agents for survivin.

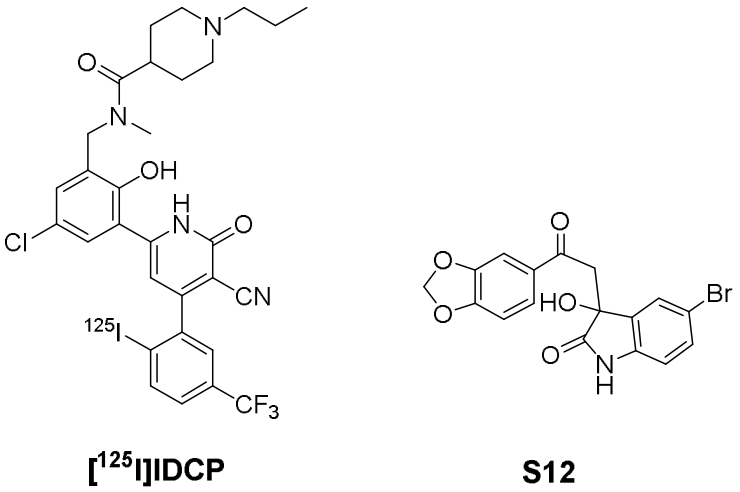


**Fig. 1.** Chemical structures of survivin-targeting small molecules.

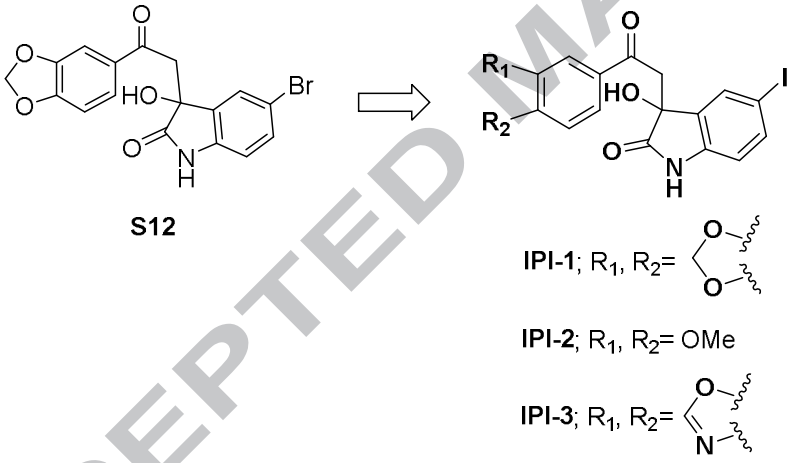


**Fig. 2.** Design of PI derivatives for their application in SPECT imaging.

## 2. Results and discussion

### 2.1. Chemistry

The synthesis of PI derivatives was accomplished according to the pathway illustrated in Schemes 1 and 2. The nucleophilic addition of 3',4'-(methilenedioxyl) acetophenone to 5-bromoisatin produced the lead compound S12. Bromo-to-tributyltin exchange reaction of 5-bromoisatin catalyzed by Pd(0) yielded tributyltin derivative **1**. Compound **2** was synthesized from compound **1** using the procedure for S12 synthesis. Finally, iodine ($I_2$)/chloroform ($CHCl_3$) solution was added to compound **2** to yield the target IPI-1 by tributyltin-to-iodine exchange reaction (Scheme 1). IPI-2 and IPI-3 could be obtained by a one-step nucleophilic addition of 3',4'-dimethoxyacetophenone or 5-acetylbenzoxazole to 5-iodoisatin (Scheme 2).

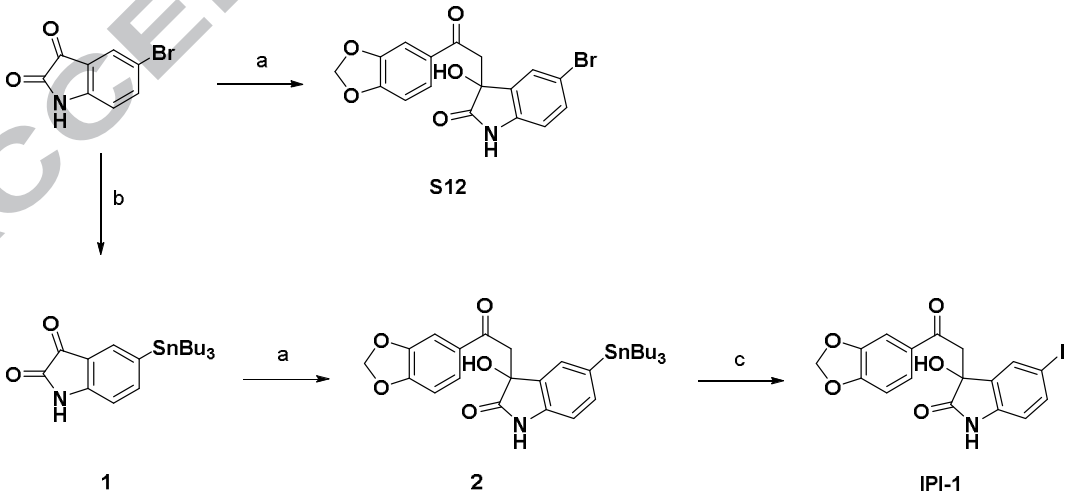

**Scheme 1.** Reagents and conditions; (a) 3',4'-(Methylenedioxy)acetophenone, MeOH, $Et_2NH_2$, r.t. 6-30 h, 21% for S12 and 22% for **2**, (b) $(Bu_3Sn)_2$, $(Ph_3P)_4Pd$, Dioxane, TEA, r.t.. 6 h, 11%. (c) $I_2$, $CHCl_3$, r.t. 2 hr,quant.

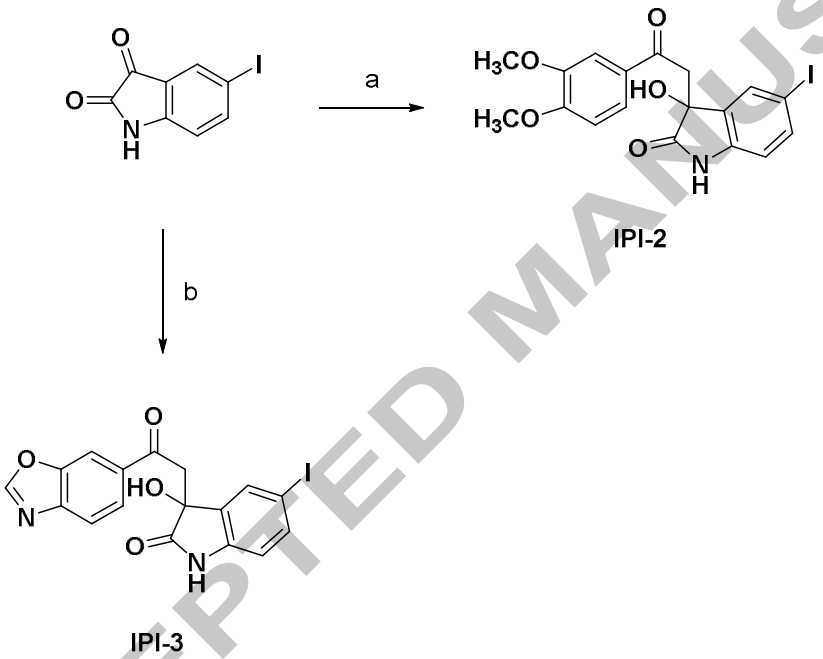


**Scheme 2.** Reagents and conditions: (a) 3',4'-dimethoxy acetophenone, $Et_2NH$, MeOH, r.t., 31 hr, 58%. (b) 5-acetylbenzoxazole $Et_2NH$, MeOH, r.t., 31 hr, 19%.

### 2.2. Evaluation of the binding of PI derivatives to survivin

The binding affinities of PI derivatives to survivin were evaluated by quartz crystal

microbalance (QCM)—a highly sensitive and accurate mass measuring technique based on the linear decrease in the resonance frequency in response to the mass increase on a QCM plate at a nanogram level.[14] This method is used to evaluate the binding affinity of small molecules to biomolecules.[15,16] Fig. 3 shows the representative QCM sensorgram of the binding interaction between IPI-1 and QCM electrodes coated with survivin. The binding of IPI-1 to survivin protein showed saturation and well-fitted one binding site model ($R_2 = 0.955$). By using the same procedure, QCM assays of S12, IPI-2, and IPI-3 were performed and similar sensorgrams were obtained (data not shown). The value of $K_d$ for each compound was calculated from the frequency changes of QCM plates, and the binding affinities of all compounds to survivin were compared. As shown in Table 1, IPI-1 showed slightly higher binding affinity ($K_d$ = 68.3 nM) as compared with lead compound S12 ($K_d$ = 77.0 nM), indicating that the substitution from bromine to iodine retains the binding affinity to survivin. On the other hand, IPI-2 and IPI-3 showed a $K_d$ value of 169 and 140 nM, respectively, indicating that the substitution of benzo[1,3]dioxolyl with dimethoxyphenyl or benzoxazolyl group at 3-position of IPI-1 resulted in a decreased binding affinity for survivin.

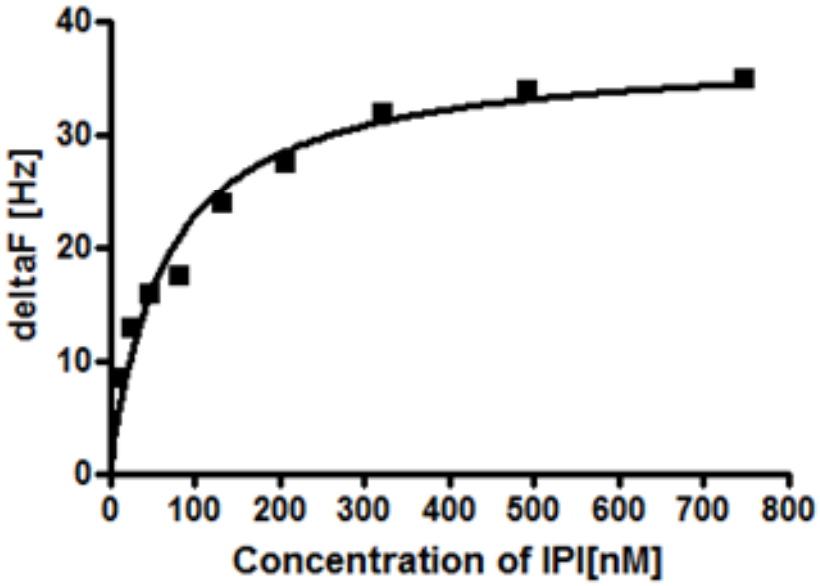


**Fig. 3.** Typical response curves of IPI-1 bound to QCM electrodes coated with survivin. The delta F value represents the frequency change of electrodes.

**Table 1.** Dissociation constant ($K_d$) of PI derivatives for survivin determined by QCM assay.

| Compounds | $K_d$[a] (nM) |
|---|---|
| **S12** | 77.0 ± 23.2 |
| **IPI-1** | 68.3 ± 2.60 |
| **IPI-2** | 169 ± 46.2 |
| **IPI-3** | 140 ± 22.6 |

*Values are mean ± SEM, n = 3.

### 2.3. *In vitro* binding assay of [$^{125}$I]IPI-1 in cell lines

Based on the results of the binding assay to recombinant survivin, we selected IPI-1 as the radioiodinated imaging agent for survivin in further experiments. The radiosynthesis of [$^{125}$I]IPI-1 was performed by an iododestannylation reaction of tributyltin derivative **2** with an oxidant chloramine T to obtain a radiochemical yield of 95% and purity of > 95% (Scheme 3). The yield of purified [$^{125}$I]IPI-1 was confirmed by analytical HPLC using the cold reference IPI-1 (Fig. 4). Next, we evaluated the binding properties of [$^{125}$I]IPI-1 to intracellular survivin using two cell lines exhibiting different expression level of survivin. MDA-MB-231 is a human breast carcinoma cell line with high survivin expression level, while MCF-10A is a human breast non-tumorigenic epithelial cell line with low expression of survivin.[17] We evaluated the *in vitro* binding of [$^{125}$I]IPI-1 to cellular survivin using fixed and permeabilized cells to abolish cell membrane permeability factors of the radioligand. As shown in Fig. 5A, [$^{125}$I]IPI-1 demonstrated a significantly higher accumulation in MDA-MB-231 cells as compared with MCF-10A cells (88.4% versus 15.3% ID/mg protein, $P < 0.05$). The binding to MDA-MB-231 cells was significantly decreased by co-incubation with 5.0

μM S12 (88.4% versus 37.2% ID/mg protein, $P < 0.05$). On the other hand, no significant blocking effect of S12 was observed in MCF-10A cells. These results indicate that the binding level of [$^{125}$I]IPI-1 corresponded to the cellular survivin expression. These results are consistent with our previous reports on [$^{125}$I]IDCP.[12] However, [$^{125}$I]IPI-1 showed higher specific binding to survivin-positive cells as compared to [$^{125}$I]IDCP. Next, we evaluated the uptake of [$^{125}$I]IPI-1 in the living cells, wherein the binding of the radioligand to the intracellular survivin relied on its cell permeability (Fig. 5B). Consistent with the results of permeabilized cells, the amount of [$^{125}$I]IPI-1 binding was significantly higher in MDA-MB-231 cells as compared with MCF-10A cells (35.9% versus 17.7% ID/mg protein, $P < 0.001$). In addition, accumulation of [$^{125}$I]IPI-1 was blocked by S12 only in MDA-MB-231 cells in a dose-dependent manner. This suggests that uptake of [$^{125}$I]IPI-1 is dependent on the expression level of survivin in living cells. The decrease in the uptake of [$^{125}$I]IPI-1 in the living cells as compared to permeabilized cells may be associated with the cell permeability, efflux,. and/or metabolism factors. Taken together, these *in vitro* results suggest that [$^{125}$I]IPI-1 displays the potential to bind specifically to survivin in living cells.

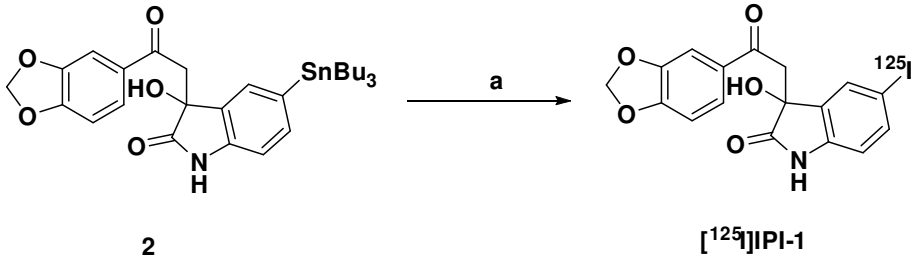


2 [$^{125}$I]IPI-1

**Scheme 3.** Reagents and conditions: (a) Na$^{125}$I, Chloramine T, 1 M HCl, EtOH, r.t., 95%.

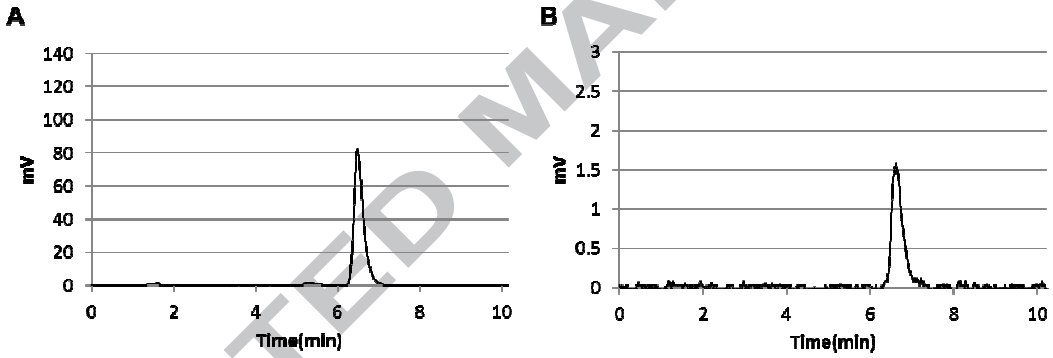


**Fig. 4.** Analytical HPLC chromatogram of UV (A) and radioactivity (B) after co-injection of purified [$^{125}$I]IPI-1 with the cold reference IPI-1.

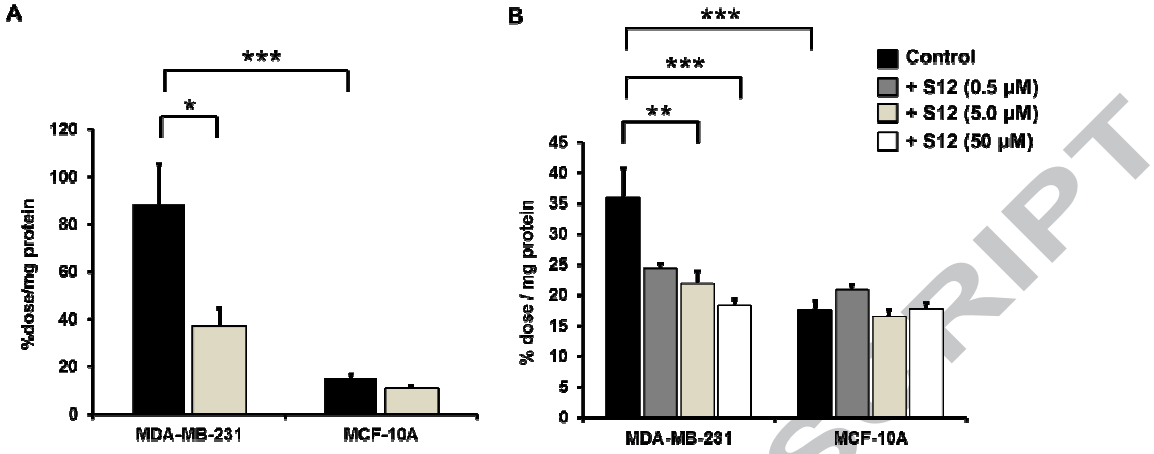


**Fig. 5.** *In vitro* binding of [$^{125}$I]IPI-1 to permeabilized (A) and living cells (B). Nonspecific binding was determined by co-incubation of S12. * $P < 0.05$, ** $P < 0.01$, *** $P < 0.001$ (ANOVA, Bonferroni t test). Data are shown as means ± SEM, n = 6 (A), n= 6-10 (B).

### 2.4. Biodistribution of [$^{125}$I]IPI-1 in tumor-bearing mice

Next, we assessed the biodistribution of [$^{125}$I]IPI-1 in BALB/c mice bearing MDA-MB-231 xenografts at 30, 60, and 180 min after tail vein injection. As shown in Table 2, the highest uptake of [$^{125}$I]IPI-1 in most organs was observed at 30 min after injection and decreased with time. Furthermore, [$^{125}$I]IPI-1 exhibited hepatobiliary excretion and its highest uptake was observed in the intestine (12.2% and 19.7% ID/g at 30 and 60 min). Uptake of [$^{125}$I]IPI-1 derivatives by the thyroid gland increased with time, which indicated gradual deiodination. The accumulation of [$^{125}$I]IPI-1 in the tumor

tissue was 1.37% ID/g at 30 min and decreased to 0.32% ID/g at 180 min. The tumor/muscle ratio of [$^{125}$I]IPI-1 increased over time and a maximum value of 2.41 was obtained at 180 min after injection. The co-injection of S12 (2.5 mg/kg) and [$^{125}$I]IPI-1 decreased the tumor uptake (1.37% versus 0.99% ID/g) and tumor/muscle ratio from 1.15 to 0.78 at 30 min. Tumor/blood ratio was less than 1.0 at all times; however, a small alteration in tumor/blood ratio was observed following co-injection with S12 (0.90 versus 0.87). Although pretreatment with S12 slightly reduced the tumor/muscle ratio, the effect of S12 on inhibition of tumor accumulation was minimal. It is possible that the S12-mediated reduction in tumor/muscle ratio was mainly caused by a reduction in circulating [$^{125}$I]IPI-1. In addition, the low tumor/blood contrast and the small inhibitory effect on [$^{125}$I]IPI-1 may be attributed to insufficient binding between IPI-1 and survivin, nonspecific cellular binding, and/or insufficient metabolic stability. The significantly reduced [$^{125}$I]IPI-1 level in the kidneys, intestines, and brain during S12 pretreatment may also be due to reduced [$^{125}$I]IPI-1 concentration in the blood. Interestingly, the tissue/blood contrast of the kidneys, intestines, and brain was not significantly different between the control and the blocking groups. On the other hand, our previous report demonstrated that [$^{125}$I]IDCP showed 0.51% ID/g of tumor uptake with 0.37 of tumor/blood at 30 min after injection.[12] In comparison with [$^{125}$I]IDCP,

[$^{125}$I]IPI-1 exhibited higher tumor uptake and contrast to non-target region, indicating that PI derivatives may exhibit superior pharmacokinetic properties as compared with DCP derivatives for *in vivo* imaging of survivin-expressing tumor tissues. Further structure-activity relationship studies are needed for the optimization of *in vivo* pharmacokinetics and to discover survivin-imaging agents with superior survivin-positive tumor targeting efficiencies and higher contrast against non-targeting tissues.

**Table 2.** Biodistribution of [$^{125}$I]IPI-1 in MDA-MB-231 tumor-bearing mice.[a]

| | Time after injection (min) | | | |
|---|---|---|---|---|
| Organ | 30 | 60 | 180 | 30 (blocking)[b] |
| | [$^{125}$I]IPI-1 | | | + S12 |
| Blood | 1.53 (0.13) | 0.82 (0.18) | 0.54 (0.06) | 1.01 (0.16)* |
| Liver | 8.82 (0.93) | 3.40 (1.27) | 1.84 (0.83) | 6.15 (2.60) |
| Kidney | 5.40 (0.77) | 1.94 (0.77) | 0.59 (0.12) | 3.51 (0.40)* |
| Intestine | 12.17 (2.04) | 19.68 (5.07) | 8.35 (0.78) | 5.38 (1.57)* |
| Spleen | 1.16 (0.18) | 0.37 (0.13) | 0.25 (0.09) | 0.81 (0.24) |

| | | | | |
|---|---|---|---|---|
| Lung | 1.97 (0.27) | 0.76 (0.16) | 0.45 (0.03) | 1.51 (0.63) |
| Stomach | 5.75 (3.90) | 3.73 (1.87) | 2.26 (0.48) | 4.71 (2.52) |
| Pancreas | 4.87 (5.09) | 0.69 (0.36) | 0.19 (0.03) | 1.71 (0.61) |
| Heart | 1.68 (0.27) | 0.48 (0.21) | 0.14 (0.01) | 1.23 (0.31) |
| Brain | 0.62 (0.05) | 0.27 (0.07) | 0.04 (0.01) | 0.45 (0.02)** |
| Thyroid | 2.08 (0.16) | 2.85 (0.23) | 11.8 (8.23) | 1.84 (0.22) |
| Muscle | 1.21 (0.21) | 0.33 (0.10) | 0.13 (0.04) | 1.13 (0.11) |
| Tumor | 1.37 (0.07) | 0.61 (0.15) | 0.32 (0.08) | 0.99 (0.41) |
| | Tumor-to-nontumor ratios | | | |
| Tumor/Blood | 0.90 (0.10) | 0.74 (0.05) | 0.57 (0.08) | 0.87 (0.20) |
| Tumor/Muscle | 1.15 (0.24) | 1.87 (0.31) | 2.41 (0.69) | 0.78 (0.21) |

[a]Expressed as % of injected dose per gram (% ID/g). Each value represents mean (SD) for three mice at each interval.

[b]Blocking group was treated with the co-injection of S12 (2.5 mg/kg) and [$^{125}$I]IPI-1.

* $P < 0.05$, ** $P < 0.01$ compared with corresponding control group (unpaired t test).

## 3. Conclusion

Here, we demonstrated the successful synthesis of PI derivatives as candidate

survivin-imaging probes. Of these, [$^{125}$I]IPI-1 displayed high binding affinity for recombinant survivin and its *in vitro* accumulation corresponded with the expression level of survivin. Biodistribution studies in tumor-bearing mice revealed moderate uptake of [$^{125}$I]IPI-1 by the tumor tissue. In addition, small inhibitory effects of S12 on tumor uptake and tumor-to-muscle ratio were observed. Therefore, although further structural modifications are necessary to improve pharmacokinetic properties of PI derivatives, this study demonstrates the feasibility with the use of PI backbone as a scaffold for the development of tumor-imaging agents targeting survivin.

## 4. Experimental

### 4.1. General information

All reagents were commercial products and used without further purification unless otherwise indicated. Na[$^{125}$]I was obtained from MuromachiYakuhin (Tokyo, Japan) or Perkin Elmer Life Sciences (Boston, MA, USA). The $^{1}$H NMR spectra was obtained using a Jeol JNMAL-400 spectrometer with TMS as the internal standard. The mass spectra were obtained using JMS－700N or JMS-T100TD instruments (JEOL, Japan). The HPLC analysis was performed by a Shimadzu HPLC system (LC-10AT pump with SPD-10A UV detector, λ= 254 nm). NaI(Tl) scintillation survey meter (TCS-172B)

manufactured by Hitachi–Aloka Medical,was used for detection of radioactivity.

An automated gamma counter with a NaI (Tl) detector (2470 WIZARD2, Perkin-Elmer) was used to measure the radioactivity. Female BALB/c nu/nu mice were purchased from Japan SLC (Hamamatsu, Japan). The experiments with animals were conducted in accordance with our institutional guidelines and were approved by the Nagasaki University Animal Care Committee.

### 4.2. Chemistry

#### 4.2.1. 3-(2Benzo[d][1,3]dioxol-5-yl)-2-oxoethyl)-5-bromo-3-hydroxyindolin-2-one (S12)

Diethylamine (0.3 mL) and 3',4'-(methilenedioxyl acetophenone) (1.64 g, 10 mmol) were added to a solution of 5-bromoisatin (1.13 g, 5.0 mmol) in methanol (MeOH; 30 mL). The mixture was stirred at room temperature for 11 h. The reaction mixture was evaporated to dryness and the residue was treated with water and extracted thrice with ethyl acetate (EtOAc). The combined organic layer was washed with brine, dried over sodium sulfate ($Na_2SO_4$), and the solvent removed. The residue was recrystallized from a mixture of dichloroethane and hexane to obtain a yellow solid of S12 (405 mg, 21%

yield). $^{1}$H NMR(DMSO-$d_6$): δ 3.53(d, *J*=17.6 Hz, 1 H), 4.07(d, *J*=17.6 Hz, 1 H), 6.12(s, 2 H), 6.77(d, *J*=8.4 Hz, 1 H), 7.02(d, *J*=8.4 Hz, 1 H), 7.32(d, *J*=1.6 Hz, 1 H), 7.34(dd, *J*=2.0, 8.4 Hz, 1 H), 7.47(d, *J*=2.0 Hz, 1 H), 7.56(dd, *J*=1.8, 8.4 Hz, 1 H). MS (DART) *m/z*: 390 $[M+H]^+$.

**4.2.2. 5-(Tributylstannyl)indoline-2,3-dione (1)**

Triethylamine (0.5 mL), bis(tributyltin) (1.2 mL, 2.40 mmol), and tetrakis(triphenylphosphine)palladium $(PPh_3)_4Pd$ (10 mg, 8.65 μmol) were added to a solution of 5-bromoisatin (180 mg, 0.80 mmol) in 1,4-dioxane (5.0 mL). The mixture was heated at 110 °C for 14 h. After the reaction mixture was cooled to room temperature, the solution was passed through celite and silica gel (1:3) and washed with EtOAc:hexane. The solvent was removed, and the crude product was chromatographed on silica gel with a 1:5 mixture of EtOAc:hexane to yield a colorless oil of **1** (38 mg, 11% yield). $^{1}$H NMR ($CDCl_3$): δ 0.89 (t, *J*= 14.4 Hz, 9H), 1.05-1.09 (m, 6 H), 1.27-1.37 (m, 6 H) 1.48-1.54 (m, 6 H), 6.88 (d, *J*=7.6 Hz, 1 H), 7.62 (d, *J*= 7.6 Hz, 1 H), 7.69 (s, 1 H). MS (DART) *m/z*: 436 $[M+H]^+$.

**4.2.3.**

**3-(2-(Benzo[d][1,3]dioxol-5-yl)-2-oxoethyl)-3-hydroxy-5-(tributylstannyl)indolin-2-one (2)**

Diethylamine (0.2 mL) and 3',4'-(methilenedioxyl acetophenone) (65 mg, 0.411 mmol) were added to the solution of **1** (60 mg, 0.137 mmol) in MeOH (3.0 mL). The mixture was stirred at room temperature for 30 h. The solvent was removed and the crude product chromatographed on silica gel with a 49:1 mixture of $CHCl_3$ and MeOH to yield a white solid of **2** (18 mg, 22% yield).$^1$H NMR ($CDCl_3$): δ 0.85 (t, *J*= 14.4 Hz, 9 H), 0.97-1.01 (m, 6 H), 1.24-1.33 (m, 6 H), 1.44-1.52 (m, 6 H), 3.42(d, *J*= 17.2 Hz, 1 H), 3.68 (d, *J*=17.2 Hz, 1 H), 6.03 (s, 2 H), 6.81 (d, *J*= 8.4 Hz, 1 H), 6.87 (d, *J*=7.6 Hz, 1 H), 7.31 (dd, *J*=1.0, 8.4 Hz, 1 H), 7.39 (d, *J*=1.6 Hz, 1 H),7.43(s,1 H), 7.49 (dd, *J*=8.0, 1.6 Hz, 1 H). MS (DART) *m/z*: 602 $[M+H]^+$.

**4.2.4. 3-(2-(Benzo[d][1,3]dioxol-5-yl)-2-oxoethyl)-3-hydroxy-5-iodoindolin-2-one (IPI-1)**

A solution of iodine in $CHCl_3$ (100 mg/mL, 1.0 mL) was added to a solution of **2** (14.9 mg) in $CHCl_3$ (1.0 mL) at room temperature. The mixture was stirred at room temperature for 2 h and then quenched by saturated aqueous sodium bisulfite ($NaHSO_3$). The aqueous layer was extracted thrice with $CHCl_3$, while the organic layer was

successively washed with saturated aqueous sodium bicarbonate ($NaHCO_3$). The organic layer was washed with brine and then dried in the presence of sodium sulfate ($Na_2SO_4$). The crude product was chromatographed on silica gel with a 30:1 mixture of $CHCl_3$:MeOH to give a pale yellow powder of IPI-1 (14 mg, quant). $^1$H NMR ($CD_3OD$): δ 3.62(d, *J*= 17.3 Hz, 1 H), 3.96 (d, *J*= 17.1 Hz, 1 H), 6.04 (s, 2 H), 6.72 (d, *J*= 8.1 Hz, 1 H), 6.89 (d, *J*=8.3 Hz, 1 H), 7.29(d, *J*= 1.2 Hz, 1 H), 7.56 (m, *J*= 16.8 Hz, 2 H), 7.59 (d, *J*= 1.48 Hz, 1 H). HRMS (FAB) m/z calcd for $C_{17}H_{12}INO_5[M+H]^+$, 437.9839; found, 437.9841.

**4.2.5. 3-(2-(3,4-dimethoxyphenyl)-2-oxoethyl)-3-hydroxy-5-iodoindolin-2-one (IPI-2)**

A solution of 5-iodoisatin (136.5 mg, 0.5 mmol) in MeOH (2.0 mL) was added to a solution of 3',4'-(dimethoxy acetophenone) (180.2 mg, 1.0 mmol) in MeOH (2.0 mL). Diethylamine was added dropwise to the solution mixture and the mixture was stirred at room temperature for 31 h. The reaction mixture was filtrated and washed with MeOH. The residue was chromatographed on silica gel with a 30:1 mixture of $CHCl_3$:MeOH to give a pale yellow solid of IPI-2 (24 mg, 58% yield).

$^1$H NMR ($CD_3OD$): δ 3.65(d, *J*= 17.2 Hz, 1 H), 3.82 (s, 3 H), 3.89 (s, 3 H), 3.99 (d,

*J*= 17.6 Hz, 1 H), 6.71 (d, *J*=8.4 Hz, 1 H), 7.01(d, *J*= 8.8 Hz, 1 H), 7.37 (d, *J*=2.0 Hz, 1 H), 7.54 (dd, *J*=2.0, 8.4 Hz, 1 H), 7.59 (d, *J*=1.6 Hz, 1 H), 7.63 (dd, *J*=2.0, 8.0 Hz, 1 H). HRMS (FAB) m/z calcd for $C_{18}H_{16}INO_5$ $[M+H]^+$, 454.0152 ; found, 454.0153.

**4.2.6. 3-(2-(benzo[d]oxazol-6-yl)-2-oxoethyl)-3-hydroxy-5-iodoindolin-2-one (IPI-3)**

A solution of 5-iodoisatin (136.5 mg, 0.5 mmol) in MeOH (2.0 mL) was added to a solution of 5-acetylbenzoxazole (161.2 mg, 1.0 mmol) in MeOH (2.0 mL). Diethylamine was added dropwise to the solution mixture and the mixture stirred at room temperature for 31 h. The reaction mixture was filtrated and washed with MeOH. The residue was chromatographed on silica gel with a 20:1 mixture of $CHCl_3$:MeOH to give a pale reddish brown solid of IPI-2 (15 mg, 19% yield).

$^1$H NMR ($CD_3OD$): δ 3.74(d, *J*= 12 Hz, 1 H), 4.10 (d, *J*= 17.6 Hz, 1 H), 6.70 (d, 8.4, 1 H), 7.51 (d, *J*= 8.4 Hz, 1 H), 7.59 (s, 1 H), 7.69 (d, *J*= 8.8 Hz, 1 H), 8.00 (d, *J*= 8.4 Hz, 1 H), 8.31 (s, 1 H), 8.52 (s, 1 H). HRMS (FAB) m/z calcd for $C_{17}H_{11}IN_2O_4$ $[M+H]^+$, 434.9842 ; found, 434.9839.

**4.2.7. Radioiodination of [$^{125}$I]IPI-1**

Chloramine-T (20 μL, 15 mg/mL), [$^{125}$I]NaI (3.7-7.4 MBq, specific activity 2200

Ci/mmol, 3 μL), and 1 M hydrochloric acid (HCl; 50 μL) were added to a solution of **2** (0.2 mg in ethanol 50 μL) in a sealed vial. The reaction was performed at room temperature for 15 min and terminated by the addition of saturated aqueous $NaHSO_3$ (100 μL). After alkalization with 100 μL of saturated $NaHCO_3$ and extraction with EtOAc, the extract was dried by passing it through an anhydrous $Na_2SO_4$ column and evaporated to dryness. The crude products were purified by high-performance liquid chromatography (HPLC) on Cosmosil C18 column (Nacalai Tesque, $5C_{18}$-AR-II, 4.6 × 250 mm) with an isocratic solvent mixture of acetonitrile ($CH_3CN$) and water (4:6) at a flow rate of 1.0 mL/min. HPLC retention time of [$^{125}$I]IPI-1 was 6.8 min, consistent with that of the corresponding non-radioactive IPI-1.

### 4.3. Saturation binding assay of PI derivatives to recombinant survivin protein

Recombinant human survivin was expressed and purified as previously described [13]. Kinetic analyses were performed with QCM system (Affinix Q, Initium Inc., Tokyo, Japan). The survivin protein (40 μg/mL) was immobilized on the gold electrode of the sensor chip via amide bonds. The sensor chip was set on QCM apparatus and soaked in a buffer. An 8 μL aliquot of 10–256 μM PI derivatives was sequentially injected into the cuvette. The changes in the frequency were monitored over time. The

kinetic analysis was performed by AQUA ver. 1.3 software (Initium Inc.).

### 4.4. Cell culture

The breast cancer cell line MDA-MB-231 and a normal immortalized human mammary epithelial cell line MCF-10A were obtained from the American Type Culture Collection (ATCC; Manassas, VA, USA). MDA-MB-231 cells were grown in Leibovitz's L-15 medium supplemented with 10% fetal bovine serum (FBS). MCF-10A were grown in Dulbecco's modified Eagle's medium (DMEM)/F-12 supplemented with 5% horse serum, 20 ng/mL epidermal growth factor (EGF), 10 μg/mL insulin, and 0.5 μg/mL hydrocortisone. All media mentioned above were supplemented with 100 IU/mL penicillin and 100 μg/mL streptomycin.

### 4.5. *In vitro* binding of [$^{125}$I]IPI-1

MDA-MB-231 and MCF-10A cells were grown to confluence on six-well plates and washed with phosphate-buffered saline (PBS). The cells were fixed with 3.7% formaldehyde and permeabilized by 0.3% Triton X. [$^{125}$I]IPI-1 in 1% dimethyl sulfoxide (DMSO)/PBS (1.0 kBq/mL, 0.5 mL) with or without S12 (5 μM) was added to the cells and incubated at 37 °C for 1 h. The cells were washed with 1% DMSO/PBS and PBS

(0.5 mL) and lysed using 0.5 M sodium hydroxide (NaOH; 200 μL) at 37 °C for 42 h. The radioactivity of the lysate was measured with gamma counter and the protein concentration was determined using the DC protein assay kit (Bio-Rad, Hercules, USA).

### 4.6. *In vitro* uptake of [$^{125}$I]IPI-1

MDA-MB-231 and MCF-10A cells were grown to confluence on six-well plates and washed with PBS. [$^{125}$I]IPI-1 dissolve in growing medium (1.0 kBq/mL, 0.5 mL) was added to each cells and incubated at 37 °C for 2 h with or without S12 (0.5, 5, 50 μM). Following incubation, cells were washed twice with 20 units heparin/PBS (0.5 mL) and lysed using 0.5 M NaOH (200 μL) at 37 °C for 18 h. The radioactivity of the lysate was measured with gamma counter and the protein concentration was determined using the DC protein assay kit.

### 4.7. Tumor xenograft model

BALB/c nu/nu mice (female, 4 weeks old) were maintained in a room with a constant ambient temperature and a 12 h light/dark cycle and had free access to food and water. Mice were subcutaneously injected on their right shoulders with

approximately $1.0 \times 10^7$ MDA-MB-231 cells. The tumors were allowed to reach 300–500 $mm^3$ (34 weeks after inoculation) before biodistribution studies were performed.

### 4.8. Biodistribution of [$^{125}$I]IPI-1 in tumor-bearing mice

[$^{125}$I]IPI-1 (10 kBq) was dissolved in 1 % DMSO saline (100 μL) and intravenously injected into the mice via the tail vein. At the designated time intervals, mice were sacrificed and their organs dissected. The tissues were weighed and the radioactivity was measured with automated gamma counting (n = 3).

### 4.9. Statistical analysis

Statistical significance was determined at $P < 0.01$ using the one-way analysis of variance (ANOVA) for comparison of more than two means, followed by the post hoc tests using Bonferroni's correction for *in vitro* experiments or unpaired t-test for *in vivo* experiments.



### Acknowledgments

Financial support was provided by a Grant-in-Aid for Young Scientists (B) (Grant

No. 21791180) and Grant-in-Aid for Scientific Research (C) from the Japan Society for the Promotion of Science (JSPS). This work was supported partly by Takeda Science Foundation, Konica Minolta Science and Technology Foundation, Mochida Memorial Foundation for Medical and Pharmaceutical Research, and SGH Foundation.

**Reference Reference**

1. Ambrosini G, Adida C, Altieri DC. *Nat. Med.*1997;3;917-921.
2. Singh N, Subramanian K, Kanwar RK, Cheung C.H., Kanwar JR, *Drug Discov. Today.* 2015;20;578-587.
3. Carrasco RA, Stamm NB, Marcusson E, Sandusky G, Iversen P, Patel BK. *Mol Cancer Ther* 2011;10:221–232.
4. Guvenc H, Pavlyukov MS, Joshi K, Kurt H, Banasavadi-Siddegowda YK, ea al. *Clin Cancer Res.* 2013;19;631-642.
5. Altieri DC. *Nat Rev Cancer.* 2008;8;61-70.
6. Mita AC, Mita MM, Nawrocki ST, Giles FJ. *Clin Cancer Res*, 2008;14;5000-5005.
7. Ling X, Cao S, Cheng Q, Keefe JT, Rustum YM, Li F. *PLoS ONE* 2012; 7: e45571.
8. Nagaraj S, Pisarev V, Kinarsky L, Sherman S, Muro-Cacho C, Altieri DC Gabrilovich DI. *J Immunother.* 2007; 30: 169–179.

9. Nakahara T, Yamanaka K, Hatakeyama S, Kita A, Takeuchi M, Kinoyama I, et al. *Anti-cancer Drugs.* 2011; 22: 454–462.

10. Zhu K, Qin H, Cha SC, Neelapu SS, Overwijk W, Lizee GA et al. *Vaccine*. 2007; 25: 7955–7961.

11. Wang Y, Liu X, Zhang Y, Liu G, Rusckowski M, Hnatowich DJ. *Nucl Med Biol.* 2007;34;47-54.

12. Fuchigami T, Mizoguchi T, Ishikawa N, Haratake M, Yoshida S, Magata Y, Nakayama M. *Bioorg Med Chem Lett*. 2016;26;999-1004.

13. Berezov A, Cai Z, Freudenberg JA, Zhang H, Cheng X, Thompson T, Murali R, Greene MI, Wang Q. *Oncogene*. **2012**;31;1938-1948.

14. Marx KA. *Biomacromolecules.* 2003;4;1099-1120.

15. Takakusagi Y1, Kuramochi K, Takagi M, Kusayanagi T, Manita D, Ozawa H, IwakiriK, Takakusagi K, Miyano Y, Nakazaki A, Kobayashi S, Sugawara F, Sakaguchi K. *Bioorg Med Chem.* 2008;16;9837-9846.

16. Kuramochi K, Miyano Y, Enomoto Y, Takeuchi R, Ishi K, Takakusagi Y, Saitoh T, Fukudome K, Manita D, Takeda Y, Kobayashi S, Sakaguchi K, Sugawara F. *Bioconjug Chem.* 2008;19;2417-2426.

17. Yang, L, Cao Z, Yan H, Wood W. C. *Cancer Res.* 2003;63;6815-6824.

**Graphical abstract**

We report here radioiodinated 3-phenethyl-2-indolinone (PI) derivatives as survivin targeting *in vivo* imaging agents for tumor imaging.